MOHAMMAD ZAMANI NEJAD *, *MEHDI JABBARI* **, *MEHDI GHANNAD* ***

A SEMI-ANALYTICAL SOLUTION OF THICK TRUNCATED CONES USING MATCHED ASYMPTOTIC METHOD AND DISK FORM MULTILAYERS

In this article, the thick truncated cone shell is divided into disk-layers form with their thickness corresponding to the thickness of the cone. Due to the existence of shear stress in the truncated cone, the equations governing disk layers are obtained based on first shear deformation theory. These equations are in the form of a set of general differential equations. Given that the truncated cone is divided into n disks, n sets of differential equations are obtained. The solution of this set of equations, applying the boundary conditions and continuity conditions between the layers, yields displacements and stresses. The results obtained have been compared with those obtained through the analytical solution and the numerical solution. For the purpose of the analytical solution, use has been made of matched asymptotic method (MAM) and for the numerical solution, the finite element method (FEM).

1. Introduction

Scientists have paid an enormous amount of attention to shells, resulting in numerous theories about their behavior of different kinds of shells. Truncated conical shells have widely been applied in many fields such as space fight, rocket, aviation, and submarine technology. The literature that addresses the stresses of thick conical shells is quite limited. Most of the existing literature deals with the stress or vibration analysis of thin conical shells and is based upon a thin shell or membrane shell theory.

Mirsky and Hermann [1], derived the solution of thick cylindrical shells of homogenous and isotropic materials, using the first shear deformation the-

---

* *Mechanical Engineering Department, Yasouj University, P. O. Box: 75914-353, Yasouj, Iran; E-mail: m.zamani.n@gmail.com*

** *Mechanical Engineering Faculty, Shahrood University of Technology, Shahrood, Iran*

*** *Mechanical Engineering Faculty, Shahrood University of Technology, Shahrood, Iran*

ory. Assuming the cone is to be long and the angle of the lateral side with a horizontal plane is great, Hausenbauer and Lee [2] without considering shear stresses obtained the radial, tangential and axial wall stresses in a thick-walled cone under internal and/or external pressure. Raju et al. [3] introduced a conical element for analysis of conical shells. Using the shear deformation theory and Frobenius series, Takashaki et al. [4], obtained the solution of free vibration of conical shells. Sundarasivarao et al. [5] analyzed a conical shell under pressure using the finite element method. Based on bending theory, Tavares [6] determined the stresses, strains, and displacements of a thin conical shell with constant thickness and axisymmetric load by the construction of a Green's function. Wu and Chiu [7] investigated thermally induced dynamic instability of laminated composite conical shells subjected to static and periodic thermal loads by means of the multiple scales method of perturbation theory. Correia et al. [8] used the finite element method (FEM) for analysis of a composite conical shell where the shear deformation theory has been used for formulation. Jane and Wu [9] studied thermo-elasticity problem in the curvilinear circular conical coordinate system. The hybrid Laplace transformation and finite difference were developed to obtain the solution of two dimensional axisymmetric coupled thermo-elastic equations. Wu et al. [10] presented the three-dimensional solution of laminated conical shells subjected to axisymmetric loadings using the method of perturbation. Eipakchi et al. [11] used the mathematical approach based on the perturbation theory, for elastic analysis a thick conical shell with varying thickness under nonuniform internal pressure. Based on first shear deformation theory and the virtual work principle, Ghannad et al. [12], have obtained an elastic solution for thick truncated conical shells. Using the tensor analysis, Nejad et al. [13] obtained a complete and consistent 3-D set of field equations to characterize the behavior of functionally graded material (FGM) thick shells of revolution with arbitrary curvature and variable thickness. The finite element method based on the Rayliegh-Ritz energy formulation is applied to obtain the elastic behavior of the functionally graded thick truncated cone [14]. Deformations and stresses inside multilayered thick-walled spheres are investigated by Borisov [15]. In the paper, each sphere is characterized by its elastic modules. Using a third-order shear deformation theory and matched asymptotic expansion (MAE) of perturbation theory, Eipakchi [16] calculated the displacements and stresses of a thick homogeneous, isotropic, and axisymmetric conical shells with varying thickness subjected to non-uniform internal pressure. Making use of first-order shear deformation theory (FSDT) and the virtual work principle, Ghannad and Nejad [17] generally derived the differential equations governing the homogenous and isotropic axisymmetric thick-walled cylinders with same boundary conditions at the two ends. Cui

et al. [18] used a new transformation for solving the governing equations of thin conical shells. The obtained equation is an ordinary differential equation with complex coefficients. Shadmehri et al. [19] proposed a semi-analytical approach to obtain the linear buckling response of conical composite shells under axial compression load. The principle of minimum total potential energy was used to obtain the governing equations and Ritz method was applied to solve them. Free vibration analysis of laminated conical shells is presented by Civalek [20]. He provided results for isotropic, orthotropic, and laminated cases for conical shells by using the numerical solution of governing differential equations of motion based on transverse shear deformation theory.

In the present study, one has the following.

(1) Based on FSDT and elasticity theory, the governing equations of thick-walled disks are derived.

(2) Thick truncated cone is divided into disks with constant thickness and constant height.

(3) With considering continuity between layers and applying boundary conditions, the governing set of differential equations with constant coefficients is solved.

(4) The results obtained for stresses and displacements are compared with the analytical solutions [14] and the solutions carried out through the FEM. Good agreement was found among the results.

2. Formulation of problem

In the FSDT, the sections that are straight and perpendicular to the mid-plane remain straight but not necessarily perpendicular after deformation and loading. In this case, shear strain and shear stress are taken into consideration.

Geometry of a thick truncated cone with thickness h, and the length L, is shown in Fig. 1. The location of a typical point m, within the shell element is as

$$\begin{cases} m : (r, x) = (R + z, x) \\ 0 \le x \le L \quad \& \quad -\dfrac{h}{2} \le z \le \dfrac{h}{2} \end{cases} \tag{1}$$

where z is the distance of typical point from the middle surface. In Eq. (1), R represents the distance of middle surface from the axial direction.

$$R = a + \frac{h}{2} - (\tan \beta) \, x \tag{2}$$

where β is half of tapering angle as

$$\beta = \tan^{-1}\left(\frac{a-b}{L}\right) \tag{3}$$
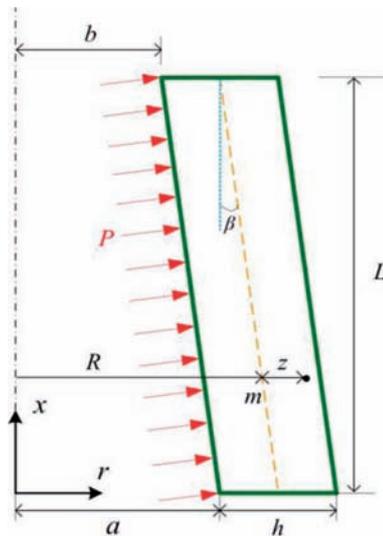
Fig. 1. Geometry of thick-walled truncated cone

Applied pressure to internal surface consists of two components as follow

$$P_x = P\sin\beta \quad , \quad P_z = P\cos\beta \tag{4}$$

where P_x and P_z are components of internal pressure P along axial and radial directions, respectively.

The general axisymmetric displacement field (U_x, U_z), in the first-order Mirsky-Hermann's theory [1] could be expressed on the basis of axial displacement and radial displacement, as follows

$$U_x(x,z) = u(x) + \phi(x)z \quad , \quad U_z(x,z) = w(x) + \psi(x)z \tag{5}$$

where $u(x)$ and $w(x)$ are the displacement components of the middle surface. Also, $\phi(x)$ and $\psi(x)$ are the functions used to determine the displacement field.

The kinematic equations (strain-displacement relations) in the cylindrical coordinates system are

$$\begin{cases} \varepsilon_x = \dfrac{\partial U_x}{\partial x} = \dfrac{du}{dx} + \dfrac{d\phi}{dx}z \\[2mm] \varepsilon_\theta = \dfrac{U_z}{r} = \left(\dfrac{w}{R+z}\right) + \left(\dfrac{\psi}{R+z}\right)z \\[2mm] \varepsilon_z = \dfrac{\partial U_z}{\partial z} = \psi \\[2mm] \gamma_{xz} = \dfrac{\partial U_x}{\partial z} + \dfrac{\partial U_z}{\partial x} = \left(\phi + \dfrac{dw}{dx}\right) + \dfrac{d\psi}{dx}z \end{cases} \tag{6}$$

The stress-strain relations (constitutive equations) for homogeneous and isotropic materials are as follows

$$\begin{Bmatrix} \sigma_x \\ \sigma_\theta \\ \sigma_z \\ \tau_{xz} \end{Bmatrix} = \lambda \begin{bmatrix} 1-\nu & \nu & \nu & 0 \\ \nu & 1-\nu & \nu & 0 \\ \nu & \nu & 1-\nu & 0 \\ 0 & 0 & 0 & \dfrac{1-2\nu}{2} \end{bmatrix} \begin{Bmatrix} \varepsilon_x \\ \varepsilon_\theta \\ \varepsilon_z \\ \gamma_{xz} \end{Bmatrix} \tag{7}$$

where σ_i and ε_i ($i = x, \theta, z$) are the stresses and strains in the axial (x), circumferential (θ), and radial (z) directions. ν and E are Poisson's ratio and modulus of elasticity, respectively. In Eq. (6), λ is

$$\lambda = \frac{E}{(1+\nu)(1-2\nu)} \tag{8}$$

The normal forces (N_x, N_θ, N_z), bending moments (M_x, M_θ, M_z), shear force (Q_x), and the torsional moment (M_{xz}) in terms of stress resultants are

$$\begin{Bmatrix} N_x \\ N_\theta \\ N_z \end{Bmatrix} = \int_{-h/2}^{h/2} \begin{Bmatrix} \sigma_x\left(1+\dfrac{z}{R}\right) \\ \sigma_\theta \\ \sigma_z\left(1+\dfrac{z}{R}\right) \end{Bmatrix} dz \tag{9}$$

$$\begin{Bmatrix} M_x \\ M_\theta \\ M_z \end{Bmatrix} = \int_{-h/2}^{h/2} \begin{Bmatrix} \sigma_x\left(1+\dfrac{z}{R}\right) \\ \sigma_\theta \\ \sigma_z\left(1+\dfrac{z}{R}\right) \end{Bmatrix} z\,dz \tag{10}$$

$$Q_x = K \int_{-h/2}^{h/2} \tau_{xz}\left(1+\frac{z}{R}\right) dz \tag{11}$$

$$M_{xz} = K \int_{-h/2}^{h/2} \tau_{xz}\left(1 + \frac{z}{R}\right)zdz \tag{12}$$

where K is the shear correction factor that is embedded in the shear stress term. In the static state, for conical shells $K = 5/6$ [21].

On the basis of the principle of virtual work, the variations of strain energy are equal to the variations of work of external forces as follows:

$$\delta U = \delta W \tag{13}$$

where U is the total strain energy of the elastic body and W is the total work of external forces due to internal pressure.

With substituting strain energy and work of external forces, we have (see [12] for a detailed description)

$$\int_0^L R(x) \int_{-h/2}^{h/2} (\sigma_x\delta\varepsilon_x + \sigma_\theta\delta\varepsilon_\theta + \sigma_z\delta\varepsilon_z + \tau_{xz}\delta\gamma_{xz})\left(1 + \frac{z}{R}\right)dzdx = $$
$$= \int_0^L (P_x\delta U_x + P_z\delta U_z)\left(R - \frac{h}{2}\right)dx \tag{14}$$

Substituting Eqs. (6) and (7) into Eq. (14), and drawing upon calculus of variation and the virtual work principle, we will have

$$\begin{cases} N_x R = -\int P_x\left(R - \frac{h}{2}\right)dx + C_0 \\[2mm] M_x\dfrac{dR}{dx} + R\left(\dfrac{dM_x}{dx} - Q_x\right) = P_x\dfrac{h}{2}\left(R - \dfrac{h}{2}\right) \\[2mm] Q_x\dfrac{dR}{dx} + R\left(\dfrac{dQ_x}{dx}\right) - N_\theta = -P_z\left(R - \dfrac{h}{2}\right) \\[2mm] M_{xz}\dfrac{dR}{dx} + R\left(\dfrac{dM_{xz}}{dx} - N_z\right) - M_\theta = P_z\dfrac{h}{2}\left(R - \dfrac{h}{2}\right) \end{cases} \tag{15}$$

and the boundary conditions are

$$\left[(N_x\delta u + M_x\delta\phi + Q_x\delta w + M_{xz}\delta\psi)\,R\right]_0^L = 0 \tag{16}$$

Eq. (16) states the boundary conditions which must exist at the two ends of the cone.

In order to solve the set of differential equations (Eqs.(15)), with using of Eqs. (6-12), and then using Eq. (15), we have

$$\begin{cases} [B_1] \dfrac{d^2}{dx^2} \{y\} + [B_2] \dfrac{d}{dx} \{y\} + [B_3] \{y\} = \{F\} \\ \{y\} = \left\{ \begin{array}{cccc} du/dx & \phi & w & \psi \end{array} \right\}^T \end{cases} \tag{17}$$

The coefficients matrices $[B_i]_{4\times4}$, and force vector $\{F\}_{4\times1}$ are as follows

$$[B_1] = \begin{bmatrix} 0 & 0 & 0 & 0 \\ 0 & (1-\nu)\dfrac{h^3}{12}R & 0 & 0 \\ 0 & 0 & \mu hR & \dfrac{\mu h^3}{12} \\ 0 & 0 & \dfrac{\mu h^3}{12} & \dfrac{\mu h^3}{12}R \end{bmatrix} \tag{18}$$

$$[B_2] = \begin{bmatrix} 0 & (1-\nu)\dfrac{h^3}{12} & 0 & 0 \\ (1-\nu)\dfrac{h^3}{12} & (1-\nu)\dfrac{h^3}{12}\dfrac{dR}{dx} & -\mu hR & -(\mu-2\nu)\dfrac{h^3}{12} \\ 0 & \mu hR & \mu h\dfrac{dR}{dx} & 0 \\ 0 & (\mu-2\nu)\dfrac{h^3}{12} & 0 & \dfrac{\mu h^3}{12}\dfrac{dR}{dx} \end{bmatrix} \tag{19}$$

$$[B_3] = \begin{bmatrix} (1-\nu)hR & 0 & \nu h & \nu hR \\ 0 & -\mu hR & 0 & 0 \\ -\nu h & \mu h\dfrac{dR}{dx} & -(1-\nu)\alpha & -h+(1-\nu)\alpha R \\ -\nu hR & 0 & -h+(1-\nu)\alpha R & -(1-\nu)\alpha R^2 \end{bmatrix} \tag{20}$$

$$\{F\} = \dfrac{1}{\lambda} \left\{ \begin{array}{c} -\int P_x\left(R-\dfrac{h}{2}\right)dx+C_0 \\ P_x\dfrac{h}{2}\left(R-\dfrac{h}{2}\right) \\ -P_z\left(R-\dfrac{h}{2}\right) \\ P_z\dfrac{h}{2}\left(R-\dfrac{h}{2}\right) \end{array} \right\} \tag{21}$$

where the parameters are as follows

$$
\begin{cases}
\mu = \dfrac{5}{12}\,(1 - 2\nu) \\[2em]
\alpha = \ln\left(\dfrac{R + \dfrac{h}{2}}{R - \dfrac{h}{2}}\right)
\end{cases}
\tag{22}
$$

The set of differential equation (Eq. (17)) is solved by matched asymptotic method (MAM) in [12]. In the next section, a new method is presented for solving set of Eqs. (15).

3. Solution with multilayer method (MLM)

In multilayer method (MLM), the truncated cone is divided into disk layers with constant thickness t, and constant height h, (Figure 2).
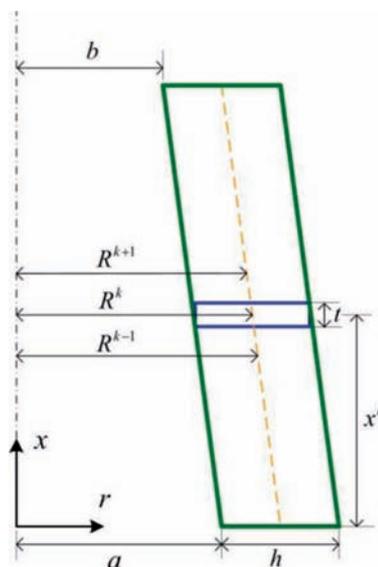
Fig. 2. Dividing of truncated cone into disk form multilayer

Therefore, the governing equations convert to nonhomogeneous set of differential equations with constant coefficients. $x^{[k]}$ and $R^{[k]}$ are length and radius of middle of disks. k is number of disks. The modulus of elasticity and Poisson's ratio of disks are assumed be constant.

The length of middle of an arbitrary disk (Figure 3) is as follows

$$\begin{cases} x^{[k]} = \left(k - \dfrac{1}{2}\right)\dfrac{L}{n} \\ \left(x^{[k]} - \dfrac{t}{2}\right) \leq x \leq \left(x^{[k]} + \dfrac{t}{2}\right) \\ t = \dfrac{L}{n} \end{cases} \qquad (23)$$

where n is the number of disks and k is the corresponding number given to each disks.

The radius of middle point of each disk is as follows

$$R^{[k]} = a + \frac{h}{2} - (\tan\beta)\, x^{[k]} \qquad (24)$$

Thus

$$\left(\frac{dR}{dx}\right)^{[k]} = \frac{dR^{[k]}}{dx^{[k]}} = -\tan\beta \qquad (25)$$
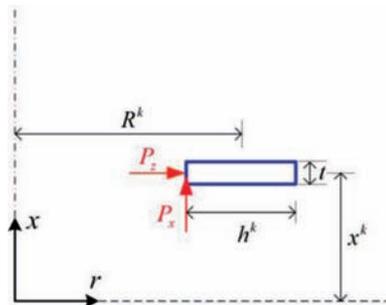
Fig. 3. Geometry of an arbitrary disk layer

With considering shear stress and based on FSDT, nonhomogeneous set of ordinary differential equations with constant coefficient of each disk is obtained.

$$\begin{cases} [B_1]^{[k]} \dfrac{d^2}{dx^2}\{y\}^{[k]} + [B_2]^{[k]} \dfrac{d}{dx}\{y\}^{[k]} + [B_3]^{[k]}\{y\}^{[k]} = \{F\}^{[k]} \\ \{y\}^{[k]} = \begin{Bmatrix} \left(\dfrac{du}{dx}\right)^{[k]} \\ \phi^{[k]} \\ w^{[k]} \\ \psi^{[k]} \end{Bmatrix} \end{cases} \qquad (26)$$

The coefficients matrices $[B_i]_{4\times4}^{[k]}$, and force vector $\{F\}_{4\times1}^k$ are as follows

$$[B_1]^{[k]} = \begin{bmatrix} 0 & 0 & 0 & 0 \\ 0 & (1-\nu)\dfrac{h^3}{12}R^{[k]} & 0 & 0 \\ 0 & 0 & \mu h R^{[k]} & \dfrac{\mu h^3}{12} \\ 0 & 0 & \dfrac{\mu h^3}{12} & \dfrac{\mu h^3}{12}R^{[k]} \end{bmatrix} \tag{27}$$

$$[B_2]^{[k]} = \begin{bmatrix} 0 & (1-\nu)\dfrac{h^3}{12} & 0 & 0 \\ (1-\nu)\dfrac{h^3}{12} & -(1-\nu)\dfrac{h^3}{12}\tan\beta & -\mu h R^{[k]} & -(\mu-2\nu)\dfrac{h^3}{12} \\ 0 & \mu h R^{[k]} & -\mu h\tan\beta & 0 \\ 0 & (\mu-2\nu)\dfrac{h^3}{12} & 0 & -\dfrac{\mu h^3}{12}\tan\beta \end{bmatrix} \tag{28}$$

$$[B_3]^{[k]} = \begin{bmatrix} (1-\nu)h R^{[k]} & 0 & \nu h & \nu h R^{[k]} \\ 0 & -\mu h R^{[k]} & 0 & 0 \\ -\nu h & -\mu h\tan\beta & -(1-\nu)\alpha^{[k]} & -h+(1-\nu)\alpha^{[k]}R^{[k]} \\ -\nu h R^{[k]} & 0 & -h+(1-\nu)\alpha^{[k]}R^{[k]} & -(1-\nu)\alpha^{[k]}\left(R^{[k]}\right)^2 \end{bmatrix} \tag{29}$$

$$\{F\}^{[k]} = \frac{1}{\lambda}\left\{ \begin{array}{c} -P\sin\beta\left(R^{[k]}-\dfrac{h}{2}\right)x + C_0 \\ \dfrac{Ph}{2}\left(R^{[k]}-\dfrac{h}{2}\right)\sin\beta \\ -P\left(R^{[k]}-\dfrac{h}{2}\right)\cos\beta \\ \dfrac{Ph}{2}\left(R^{[k]}-\dfrac{h}{2}\right)\cos\beta \end{array} \right\} \tag{30}$$

where the parameters are as follows

$$\alpha^{[k]} = \ln\left(\frac{R^{[k]}+\dfrac{h}{2}}{R^{[k]}-\dfrac{h}{2}}\right) \tag{31}$$

Defining the differential operator $P(D)$, Eq. (26) is written as

$$\begin{cases} [P(D)]^{[k]} = [B_1]^{[k]}D^2 + [B_2]^{[k]}D + [B_3]^{[k]} \\ D^2 = \dfrac{d^2}{dx^2} \quad , \quad D = \dfrac{d}{dx} \end{cases} \tag{32}$$

Thus

$$[P(D)]^{[k]} \{y\}^{[k]} = \{F\}^{[k]} \tag{33}$$

The above differential Eq. has the total solution including general solution for homogeneous case $\{y\}_h^{[k]}$ and particular solution $\{y\}_p^{[k]}$, as follows:

$$\{y\}^{[k]} = \{y\}_h^{[k]} + \{y\}_p^{[k]} \tag{34}$$

For the general solution for homogeneous case, $\{y\}_h^{[k]} = \{V\}^{[k]} e^{m^{[k]}x}$ is substituted in $[P(D)]^{[k]} \{y\}^{[k]} = 0$.

$$\left| m^2 [B_1]^{[k]} + m [B_2]^{[k]} + [B_3]^{[k]} \right| = 0 \tag{35}$$

Thus

$$\begin{vmatrix} B_{11} & B_{12} & B_{13} & B_{14} \\ B_{21} & B_{22} & B_{23} & B_{24} \\ B_{31} & B_{32} & B_{33} & B_{34} \\ B_{41} & B_{42} & B_{43} & B_{44} \end{vmatrix} = 0 \tag{36}$$

$$B_{11} = (1 - v) h R^{[k]} \tag{37}$$

$$B_{12} = B_{21} = m (1 - v) \frac{h^3}{12} \tag{38}$$

$$B_{13} = -B_{31} = vh \tag{39}$$

$$B_{14} = -B_{41} = vh R^{[k]} \tag{40}$$

$$B_{22} = m^2 (1 - v) \frac{h^3}{12} R^{[k]} - m (1 - v) \frac{h^3}{12} \tan \beta - \mu h R^{[k]} \tag{41}$$

$$B_{23} = -m \mu h R^{[k]} \tag{42}$$

$$B_{24} = -B_{42} = -m (\mu - 2v) \frac{h^3}{12} \tag{43}$$

$$B_{32} = m \mu h R^{[k]} - \mu h \tan \beta \tag{44}$$

$$B_{33} = m^2 \mu h R^{[k]} - m \mu h \tan \beta - (1 - v) \alpha^{[k]} \tag{45}$$

$$B_{34} = B_{43} = m^2 \frac{\mu h^3}{12} - h + (1 - v) \alpha^{[k]} R^{[k]} \tag{46}$$

$$B_{44} = m^2 \frac{\mu h^3}{12} R^{[k]} - m \frac{\mu h^3}{12} \tan \beta - (1 - v) \alpha^{[k]} \left(R^{[k]} \right)^2 \tag{47}$$

The result of the determinant above is a six-order polynomial which is a function of m, the solution of which are 6 eigenvalues m_i. The eigenvalues

are 3 pairs of conjugated root. Substituting the calculated eigenvalues in following equation, the corresponding eigenvectors $\{V\}_i$ are obtained.

$$\left[m^2 \, [B_1]^{[k]} + m \, [B_2]^{[k]} + [B_3]^{[k]} \right] \{V\}^{[k]} = 0 \qquad (48)$$

Therefore, the homogeneous solution for is

$$\{y\}_h^{[k]} = \sum_{i=1}^{6} C_i^{[k]} \{V\}_i^{[k]} \, e^{m_i^{[k]} x} \qquad (49)$$

The particular solution is obtained as follows

$$\{y\}_p^{[k]} = \left[[B_3]^{[k]} \right]^{-1} \{F\}^{[k]} \qquad (50)$$

Therefore, the total solution for is

$$\{y\}^{[k]} = \sum_{i=1}^{6} C_i^{[k]} \{V\}_i^{[k]} \, e^{m_i^{[k]} x} + \left[[B_3]^{[k]} \right]^{-1} \{F\}^{[k]} \qquad (51)$$

In general, the problem for each disk consists of 8 unknown values of C_i, including C_0 (Eq. (15)), C_1 to C_6 (Eq. (51)), and C_7 (equation $u^{[k]} = \int (du/dx)^{[k]} \, dx + C_7$).

4. Boundary and continuity conditions

4.1. Boundary conditions

In this problem, the boundary conditions of cone is clamped-clamped ends, then we have

$$\left\{ \begin{array}{c} u \\ \phi \\ w \\ \psi \end{array} \right\}_{x=0} = \left\{ \begin{array}{c} u \\ \phi \\ w \\ \psi \end{array} \right\}_{x=L} = \left\{ \begin{array}{c} 0 \\ 0 \\ 0 \\ 0 \end{array} \right\} \qquad (52)$$

Therefore

$$\left\{ \begin{array}{c} U_x (x, z) \\ U_z (x, z) \end{array} \right\}_{x=0,L} = \left\{ \begin{array}{c} 0 \\ 0 \end{array} \right\} \qquad (53)$$

4.2. Continuity conditions

Because of continuity and homogeneity of the cone, at the boundary between two layers, forces, stresses and displacements must be continuous.

Given that shear deformation theory applied is an approximation of one order and also all equations related to the stresses include the first derivatives of displacement, the continuity conditions are as follows

$$\left\{ \begin{array}{l} U_x^{[k-1]}(x,z) \\ U_z^{[k-1]}(x,z) \end{array} \right\}_{x=x^{[k-1]}+\frac{t}{2}} = \left\{ \begin{array}{l} U_x^{[k]}(x,z) \\ U_z^{[k]}(x,z) \end{array} \right\}_{x=x^{[k]}-\frac{t}{2}} \tag{54}$$

$$\left\{ \begin{array}{l} U_x^{[k]}(x,z) \\ U_z^{[k]}(x,z) \end{array} \right\}_{x=x^{[k]}+\frac{t}{2}} = \left\{ \begin{array}{l} U_x^{[k+1]}(x,z) \\ U_z^{[k+1]}(x,z) \end{array} \right\}_{x=x^{[k+1]}-\frac{t}{2}} \tag{55}$$

and

$$\left\{ \begin{array}{l} \dfrac{dU_x^{[k-1]}(x,z)}{dx} \\ \dfrac{dU_z^{[k-1]}(x,z)}{dx} \end{array} \right\}_{x=x^{[k-1]}+\frac{t}{2}} = \left\{ \begin{array}{l} \dfrac{dU_x^{[k]}(x,z)}{dx} \\ \dfrac{dU_z^{[k]}(x,z)}{dx} \end{array} \right\}_{x=x^{[k]}-\frac{t}{2}} \tag{56}$$

$$\left\{ \begin{array}{l} \dfrac{dU_x^{[k]}(x,z)}{dx} \\ \dfrac{dU_z^{[k]}(x,z)}{dx} \end{array} \right\}_{x=x^{[k]}+\frac{t}{2}} = \left\{ \begin{array}{l} \dfrac{dU_x^{[k+1]}(x,z)}{dx} \\ \dfrac{dU_z^{[k+1]}(x,z)}{dx} \end{array} \right\}_{x=x^{[k+1]}-\frac{t}{2}} \tag{57}$$

Given the continuity conditions, in terms of z, 8 equations are obtained. In general, if the cone is divided into n disk layers, $8(n-1)$ equations are obtained. Using the 8 equations of boundary condition, $8n$ equations are obtained. The solution of these equations yields $8n$ unknown constants.

5. Results and discussion

The solution described in the preceding section for a homogeneous and isotropic truncated conical shell with $a = 40$ mm, $b = 30$ mm, $h = 20$ mm and $L = 400$ mm will be considered. The Young's Modulus and Poisson's ratio, respectively, have values of $E = 200$ GPa and $v = 0.3$. The applied internal pressure is 80 MPa. The truncated cone has clamped-clamped boundary conditions.

The effect of the number of disk layers on the radial displacement is shown in Figure 4. It is observed that if number of disk layers is fewer than 30, it will have a significant effect on the response. However, if the number of layers is more than 40 disks, there will be no significant effect on radial displacement. In the problem in question 60 disks are used.
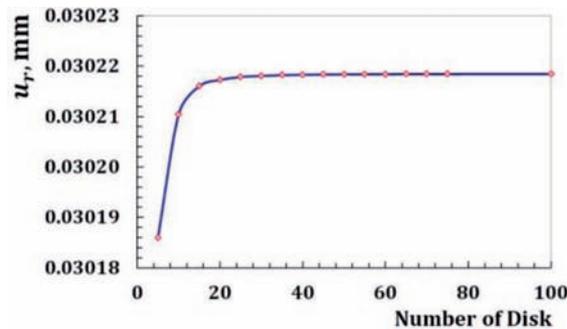
Fig. 4. Effect of the number of disk layers on the radial displacement

Figure 5 shows the distribution of axial displacement at different layers. At points away from the boundaries, axial displacement does not show significant differences in different layers, while at points near the boundaries, the reverse holds true.
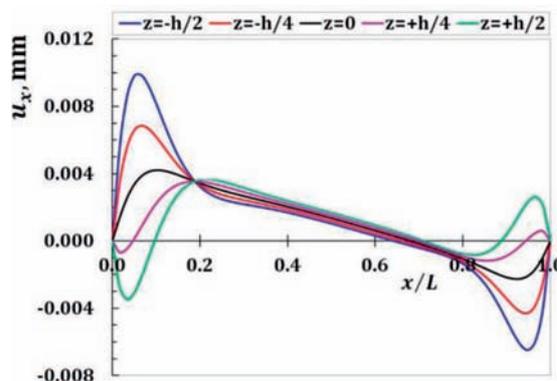
Fig. 5. Axial displacement distribution in different layers

The distribution of radial displacement at different layers is plotted in Figure 6. The radial displacement at points away from the boundaries depends on radius and length.

According to Figures 5 and 6, the change in axial and radial displacements in the lower boundary is greater than that of the upper boundary and the greatest axial and radial displacement occurs in the internal surface ($z = -h/2$). Distribution of circumferential stress in different layers is shown in Figure 7. The circumferential stress at all points depends on radius and length. The circumferential stress at layers close to the external surface is negative, and at other layers positive. The greatest circumferential stress occurs in the internal surface ($z = -h/2$). Figure 8 shows the distribution of shear stress at different layers. The shear stress at points away from the boundaries at different layers is the same and trivial. However, at points near

the boundaries, the stress is significant, especially in the internal surface, which is the greatest.
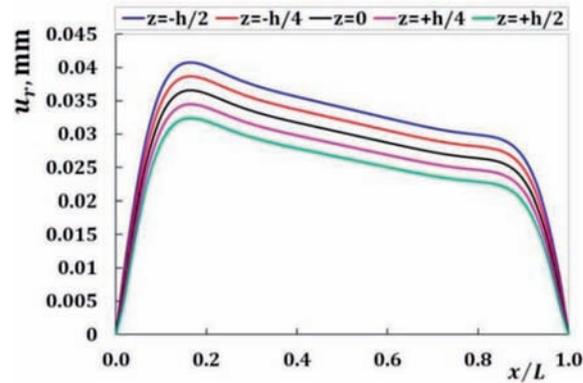
Fig. 6. Radial displacement distribution in different layers
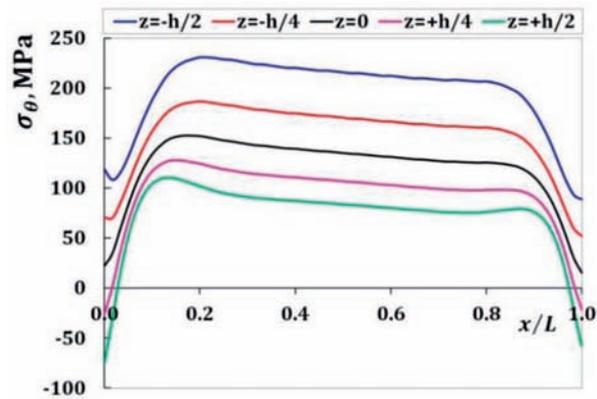
Fig. 7. Circumferential stress distribution in different layers
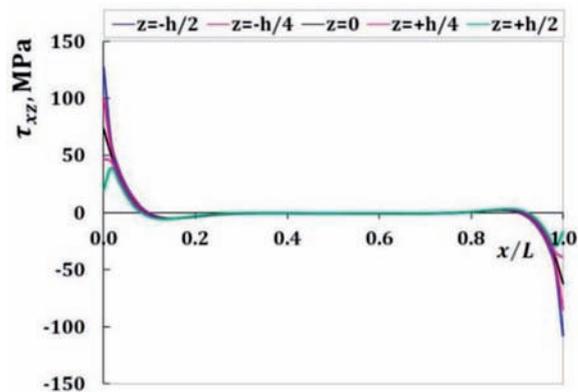
Fig. 8. Shear stress distribution in different layers

In Figures 9-13, displacement and stress distributions are obtained using MLM are compared with the solutions of FEM and are presented in the form of graphs. Figures 9 to 13 show that the disk layer method based on FSDT has an acceptable amount of accuracy when one wants to obtain radial displacement, radial stress and circumferential stress. However, they are not that useful for axial stress and not useful at all for radial displacement. It is possible to compensate for this by increasing the order of shear deformation theory. In Table 1, the values of stresses and displacements resulting from analysis of thick truncated conical shell r through MLM, MAM and FEM for clamped-clamped condition under uniform internal pressure in the middle layer are given.
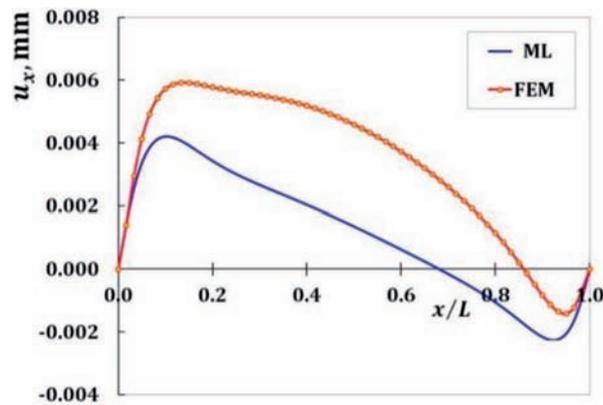
Fig. 9. Axial displacement distribution in middle layer
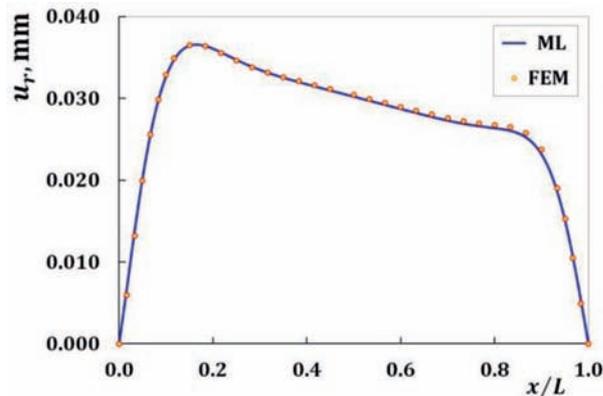
Fig. 10. Radial displacement distribution in middle layer
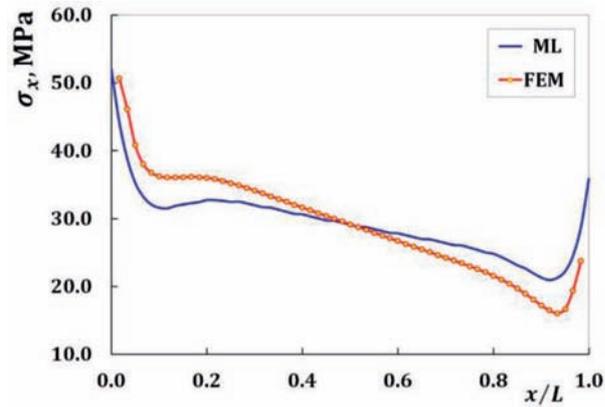
Fig. 11. Axial stress distribution in middle layer
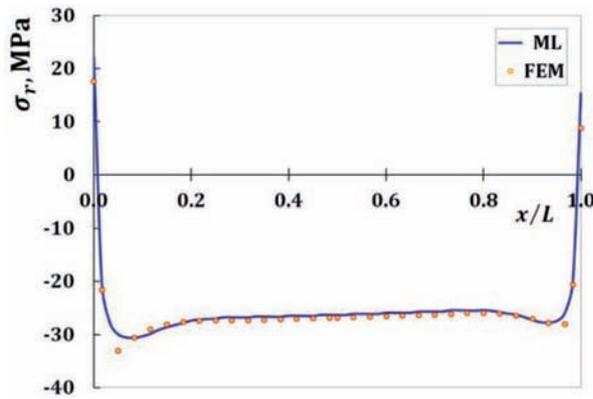
Fig. 12. Radial stress distribution in middle layer
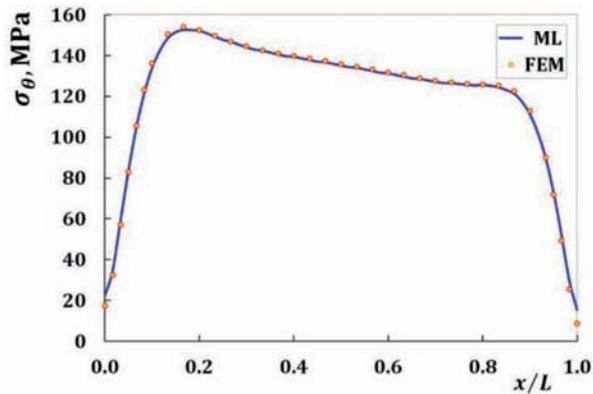
Fig. 13. Circumferential stress distribution in middle layer

6. Conclusions

Homogenous and isotropic thick-walled conical shells could be solved using the analytical method. First shear deformation theory and perturbation

Table 1.

Comparison of values of MLM, FEM and MAM

Method	u_r, mm	u_x, mm	σ_r, MPa	σ_x, MPa	σ_θ, MPa
MLM	0.03022	0.00136	-26.31	29.11	135.14
FEM	0.03041	0.00460	-26.83	29.18	135.85
MAM	0.03021	0.00400	-26.31	29.20	135.16

theory result in the analytical solution of the problem with higher accuracy and within a shorter period of time. However, the above-mentioned solutions are complicated and time-consuming. The multilayer disc form method could be a good replacement for the analysis of thick-walled shells. In this method, shells with different geometries and different loadings and different boundary conditions, with even variable pressure, could be more easily solved. This in spite of the fact that the existing analytical methods, due to their complex mathematical relations governing them, could not easily solve them. The method presented is very suitable for the purpose of calculation of radial stress, circumferential stress, shear stress and radial displacement.

REFERENCES

[1] Mirsky I., Hermann G.: Axially motions of thick cylindrical shells. Journal of Applied Mechanics-Transactions of the ASME, 1958, 25, pp. 97-102.

[2] Hausenbauer G. F., Lee G. C.: Stresses in thick-walled conical shells. Nuclear Engineering and Design, 1966, 3, pp. 394-401.

[3] Raju I. S., Rao G. V., Rao B. P., Venkataramana J.: A conical shell finite element. Computers & Structures, 1974, 4, pp. 901-915.

[4] Takahashi S., Suzuki K., Kosawada T.: Vibrations of conical shells with variable thickness. Bulletin of the JSME-Japan Society of Mechanical Engineers, 1986, 29, pp. 4306-4311.

[5] Sundarasivarao B. S. K., Ganesan N.: Deformation of varying thickness of conical shells subjected to axisymmetric loading with various end conditions. Engineering Fracture Mechanics, 1991, 39, pp. 1003-1010.

[6] Tavares S.A.: Thin conical shells with constant thickness and under axisymmetric load. Computational Structures, 1996, 60, pp. 895-921.

[7] Wu C. P., Chiu S. J.: Thermally induced dynamic instability of laminated composite conical shells. International Journal of Solids Structures, 2002, 39, pp. 3001-3021.

[8] Correia I. F. P., Soares C. M. M., Soares C. A. M., Herskovits J.: Analysis of laminated conical shell structures using higher order models. Composite Structures, 2003, 62, pp. 383-390.

[9] Jane K. C., Wu Y. H.: A generalized thermoelasticity problem of multilayered conical shells. International Journal of Solids and Structures, 2004, 41, pp. 2205-2233.

[10] Wu C. P., Pu Y. F., Tsai Y. H.: Asymptotic solutions of axisymmetric laminated conical shells. Thin-Wall Structures, 2005, 43, pp. 1589-1614.

[11] Eipakchi H. R., Khadem S. E., Rahimi G. H.: Axisymmetric stress analysis of a thick conical shell with varying thickness under nonuniform internal pressure. Journal of Engineering Mechanics-ASCE, 2008, 135, pp. 601-610.

[12] Ghannad M., Nejad M. Z., Rahimi G. H.: Elastic solution of axisymmetric thick truncated conical shells based on first-order shear deformation theory. Mechanika, 2009, 79, pp. 13-20.

[13] Nejad M. Z., Rahimi G. H., Ghannad M.: Set of field equations for thick shell of revolution made of functionally graded materials in curvilinear coordinate system. Mechanika, 2009, 77, pp. 18-26.

[14] Asemi K., Akhlaghi M., Salehi M., Zad S. K. H.: Analysis of functionally graded thick truncated cone with finite length under hydrostatic internal pressure. Archive of Applied Mechanics, 2010, 81, pp. 1063-1074.

[15] Borisov A. V.: Elastic analysis of multilayered thick-walled spheres under external load. Mechanika, 2010, 84, pp. 28-32.

[16] Eipakchi H. R.: Third-order shear deformation theory for stress analysis of a thick conical shell under pressure. Journal of Mechanics of Materials and Structures, 2010, 5, pp. 1-17.

[17] Ghannad M., Nejad M. Z.: Elastic analysis of pressurized thick hollow cylindrical shells with clamped-clamped ends. Mechanika, 2010, 85, pp. 11-18.

[18] Cui W., Pei J., Zhang W.: A simple and accurate solution for calculating stresses in conical shells. Computers & Structures, 2011, 79, pp. 265-279.

[19] Shadmehri F., Hoa S. V., Hojjati M.: Buckling of conical composite shells. Composite Structures, 2012, 94, pp. 787-792.

[20] Civalek O.: Vibration analysis of laminated composite conical shells by the method of discrete singular convolution based on the shear deformation theory. Composites Part B-Engineering, 2013, 45, pp. 1001-1009.

[21] Vlachoutsis S.: Shear correction factors for plates and shells. International Journal for Numerical Methods in Engineering, 1992, 33, pp. 1537-1552.

Półanalityczne rozwiązanie dla grubościennej powłoki stożka ściętego wykorzystujące dopasowaną metodę asymptotyczną i podział na warstwy krążkowe

S t r e s z c z e n i e

Grubościenna powłoka stożka ciętego, opisana w artykule, jest dzielona na warstwy w formie krążków o grubości odpowiadającej grubości powłoki. Ponieważ w stożku ściętym istnieją naprężenia ścinające, równania dla warstw krążkowych są otrzymane na bazie teorii odkształceń pierwszego rzędu. Równania te mają postać układu ogólnych równań różniczkowych. Zakładając, że stożek ścięty jest podzielony na *n* warstw, uzyskuje się układ *n* równań różniczkowych. Wartości przemieszczeń i naprężeń otrzymuje się w wyniku rozwiązania tego układu równań, przy uwzględnieniu warunków brzegowych i warunków ciągłości. Uzyskane wyniki porównano z wynikami rozwiązań analitycznego oraz numerycznego. Dla potrzeb rozwiązania analitycznego wykorzystano dopasowaną metodę asymptotyczną (*Matched Asymptotic Method, MAM*), a w rozwiązaniu numerycznym zastosowano metodę elementów skończonych (FEM).